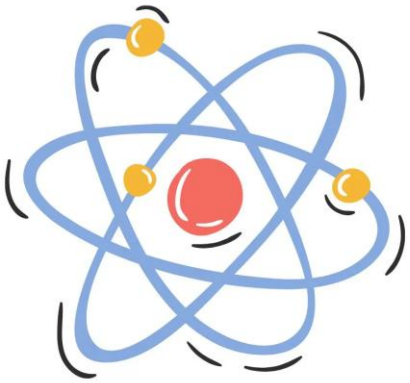

ISSN: 1672 - 6553

JOURNAL OF DYNAMICS AND CONTROL

VOLUME 10 ISSUE 01: P177 - 189

TRIBOLOGICAL PERFORMANCE OF IN-SITU AL–MG_2SI METAL MATRIX COMPOSITES UNDER DRY SLIDING CONDITIONS

Suresh K.[1], Gangadhar Medleri[2], Shubha T. C.[1]

[1]Department of Mechanical Engineering, Government Engineering College, Talakal, Koppal (Affiliated to Visvesvaraya Technological University, Belagavi),

[2]Supinco Automation PVT LTD, Bengaluru

JOURNAL OF DYNAMICS AND CONTROL
https://doi.org/10.71058/jodac.v10i01010

TRIBOLOGICAL PERFORMANCE OF IN-SITU Al–Mg_2Si METAL MATRIX COMPOSITES UNDER DRY SLIDING CONDITIONS

Suresh K.[1], Gangadhar Medleri[2], Shubha T. C.[1]

[1]Department of Mechanical Engineering, Government Engineering College, Talakal, Koppal (Affiliated to Visvesvaraya Technological University, Belagavi),
[2]Supinco Automation PVT LTD, Bengaluru

Abstract: *The dry sliding wear behavior of in-situ Al–Mg_2Si metal matrix composites was investigated at a sliding velocity of 2 m/s using a pin-on-disc configuration. Wear tests were conducted under varying normal loads using pins of 8 mm and 10 mm diameter. Wear rate, specific wear rate, coefficient of friction, frictional force, and dimensionless wear coefficient were evaluated to understand the influence of load and pin geometry at higher sliding speed. The results show that wear rate increases with increasing load, while specific wear rate remains nearly constant, indicating a stable wear mechanism consistent with Archard's law. The coefficient of friction exhibits marginal variation with load, suggesting steady-state sliding conditions. A comparative assessment reveals that the 10 mm diameter pins exhibit improved wear resistance and lower wear coefficients due to reduced contact stress. The findings confirm that applied load remains the dominant factor governing wear behavior even at higher sliding velocity, highlighting the suitability of Al–Mg_2Si composites for high-speed tribological applications.*

Keywords: *Al–Mg_2Si composites; dry sliding wear; sliding velocity; coefficient of friction; Archard's law*

1. Introduction

Aluminium and its alloys are extensively used in tribological components owing to their low density, good thermal conductivity, and ease of processing. However, their relatively poor wear resistance under dry sliding conditions limits their application in high-load and high-speed environments [1–4]. To overcome this limitation, aluminium matrix composites (AMCs) reinforced with hard ceramic or intermetallic phases have been developed to improve resistance to material removal while retaining lightweight characteristics [5–7].

Particulate-reinforced AMCs exhibit enhanced wear performance due to load transfer from the matrix to the reinforcement and restriction of plastic deformation at the contact interface [8,9]. Among the various reinforcement systems, in-situ synthesized composites have gained considerable attention because they provide cleaner interfaces, finer particle distribution, and improved thermodynamic stability compared to ex-situ reinforced systems [10–12]. The in-situ Al–Mg_2Si composite system is particularly attractive as Mg_2Si possesses low density, high hardness, good thermal stability, and excellent compatibility with the aluminium matrix [11,24].

https://doi.org/10.71058/jodac.v10i01010

Extensive tribological studies on aluminium alloys and AMCs have demonstrated that applied load is the dominant parameter influencing wear behavior. According to Archard's wear law, wear volume increases linearly with normal load under steady-state conditions, provided the wear mechanism remains unchanged [13]. Experimental investigations on aluminium alloys and particulate-reinforced AMCs consistently report a monotonic increase in wear rate with increasing load, primarily due to enlargement of the real contact area and enhanced plastic deformation of surface asperities [15–18]. Wear mechanism maps proposed by Lim and Ashby further indicate that increasing load promotes a transition from mild to severe wear regimes depending on material properties and operating conditions [16].

Despite the increase in wear rate, several studies have shown that the specific wear rate often remains nearly constant over a wide range of applied loads [19–23]. This behavior has been attributed to proportional increases in wear volume with load, resulting in load-independent specific wear rates when normalized by sliding distance and normal force. Such trends have been widely reported for aluminium alloys and aluminium-based composites under dry sliding conditions, validating the applicability of Archard's law [21–23].

Sliding velocity is another critical parameter governing tribological performance, as it influences frictional heating, oxidation kinetics, and subsurface deformation [19,26]. At higher sliding velocities, friction-induced temperature rise can soften the aluminium matrix, leading to increased wear, while in some cases the formation of protective oxide layers or mechanically mixed tribolayers stabilizes friction and limits excessive material removal [27,28]. Studies on AMCs have reported that wear rate and frictional force tend to increase with sliding velocity, whereas specific wear rate and wear coefficient often exhibit weak sensitivity to velocity within moderate speed ranges [19,26].

In addition to operating parameters, contact geometry plays an important role in determining wear behavior. Larger pin diameters reduce nominal contact stress, thereby lowering subsurface plastic deformation and crack initiation during sliding [29,30]. Comparative studies on pin-on-disc configurations have demonstrated that specimens with larger contact areas generally exhibit lower wear rates and wear coefficients under identical loading conditions [29,30]. However, limited systematic studies exist on the combined influence of pin diameter and higher sliding velocity on the tribological performance of in-situ Al–Mg_2Si composites.

Based on the above literature, it is evident that while the wear behavior of aluminium-based composites has been widely investigated, focused studies addressing the effect of contact geometry at elevated sliding velocities remain scarce. The present work aims to address this gap by systematically investigating the dry sliding wear behavior of in-situ Al–Mg_2Si metal matrix composites at a sliding velocity of 2 m/s, with particular emphasis on the influence of applied load and pin diameter on wear rate, specific wear rate, coefficient of friction, and wear coefficient.

https://doi.org/10.71058/jodac.v10i01010

The findings provide valuable insights into the suitability of Al–Mg_2Si composites for high-speed tribological applications.

2. Materials and Methods

The in-situ Al–Mg_2Si metal matrix composite used in this study was fabricated through controlled solidification of an aluminium alloy melt containing magnesium and silicon additions. The chemical composition was selected to promote in-situ formation of Mg_2Si reinforcement during solidification. Cylindrical pins of 8 mm and 10 mm diameter were machined from the cast composite, with a constant length maintained for all specimens.

Dry sliding wear tests were conducted using a pin-on-disc tribometer in accordance with ASTM G99 standards. The counterface disc was made of hardened steel with a uniform surface finish. All experiments were performed at a constant sliding velocity of 2 m/s, while the applied normal load was varied from 10 N to 100 N. The photograph of the wear testing facilities at the laboratory is shown in Figure 1. Prior to testing, the pin surfaces were polished and cleaned with acetone to remove contaminants. Each test was conducted for a fixed sliding distance under ambient laboratory conditions.

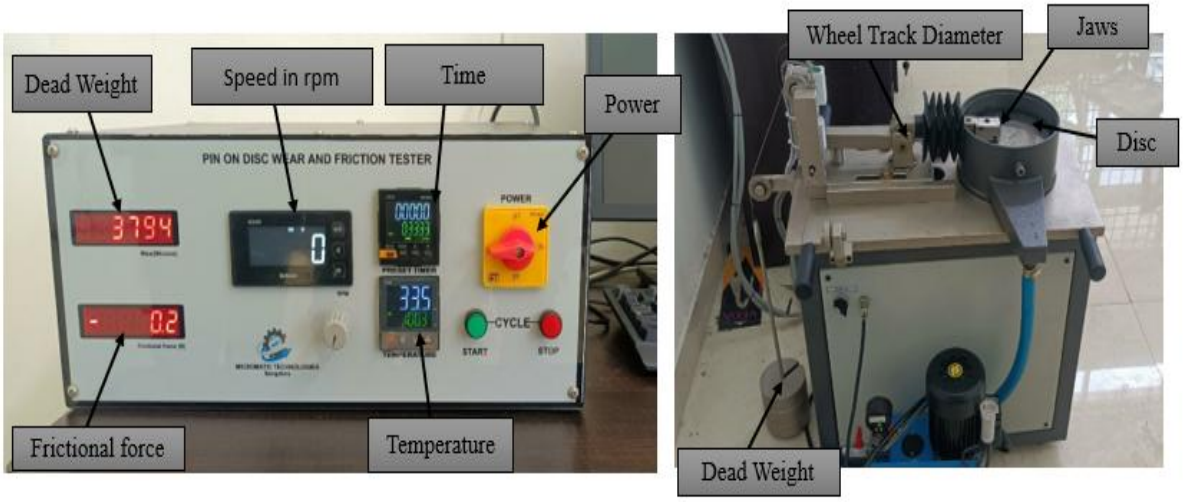

Figure 1: Photograph of the wear testing setup

3. Wear Measurement and Calculations

The wear behavior was quantified by measuring the mass loss of the specimens before and after each test using a precision balance. The corresponding volume loss was calculated using the measured density of the composite. Wear rate was determined as the volume loss per unit sliding distance. The specific wear rate was calculated by normalizing the wear rate with respect to applied load and sliding distance, following Archard's wear model [19].

https://doi.org/10.71058/jodac.v10i01010

The average frictional force was recorded continuously during the test, and the coefficient of friction was calculated as the ratio of frictional force to applied normal load. The dimensionless wear coefficient was estimated using the standard Archard equation, enabling comparison of wear performance across different test conditions.

4. Results and Discussion

This section presents a detailed analysis of the wear behavior of the composite by evaluating wear rate, specific wear rate, coefficient of friction, and dimensionless wear coefficient, and correlating these parameters with applied normal load under dry sliding conditions with velocity 2 m/s.

4.1 Wear analysis of 8 mm diameter pin specimen

The following discussion focuses on the trends observed for the 8 mm diameter pin specimen tested at a sliding velocity of 2 m/s.

Figure 2 illustrates the variation of wear rate with applied load. As the load increased from 10 N to 100 N, the wear rate increased from 0.001962 mm³/m to 0.003923 mm³/m, exhibiting a nearly linear trend. This behavior can be attributed to the increase in real area of contact between the mating surfaces due to plastic deformation of surface asperities under higher normal loads. The increased real contact area results in higher interfacial shear stresses, which facilitate material removal from the comparatively softer matrix during sliding, leading to an increased wear rate.

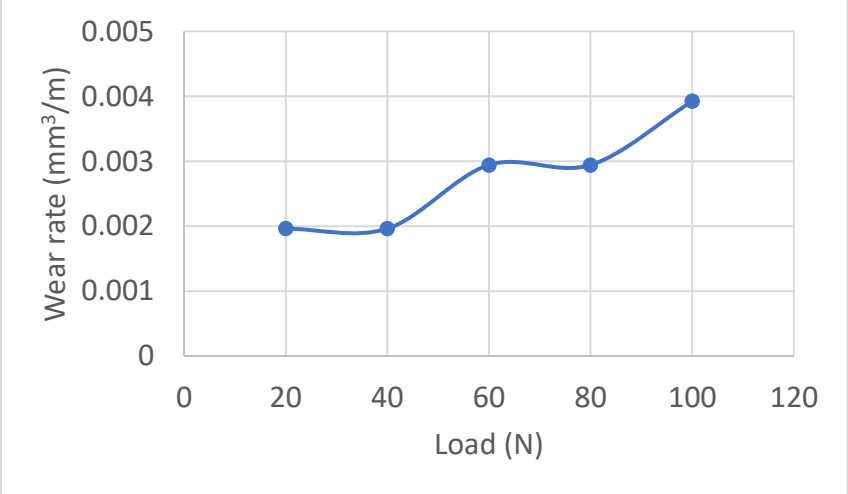

Figure 2: Wear rate vs load for 8 mm specimen at 2 m/s

The variation of specific wear rate with load is shown in Figure 3. At lower loads (10–20 N), the specific wear rate exhibits higher values, approximately 9.81×10^{-5} mm³/Nm, which may be attributed to the initial running-in period characterized by unstable contact conditions and higher material removal. With further increase in load, the specific wear rate remains nearly constant,

https://doi.org/10.71058/jodac.v10i01010

varying only between 3.68×10^{-5} and 4.9×10^{-5} mm³/Nm up to 100 N. This behavior is consistent with Archard's wear law, which states that wear volume is directly proportional to the applied load under mild wear conditions. When the wear volume increases linearly with load, normalization with respect to load and sliding distance results in an approximately constant specific wear rate, indicating that the dominant wear mechanism remains unchanged within the investigated load range.

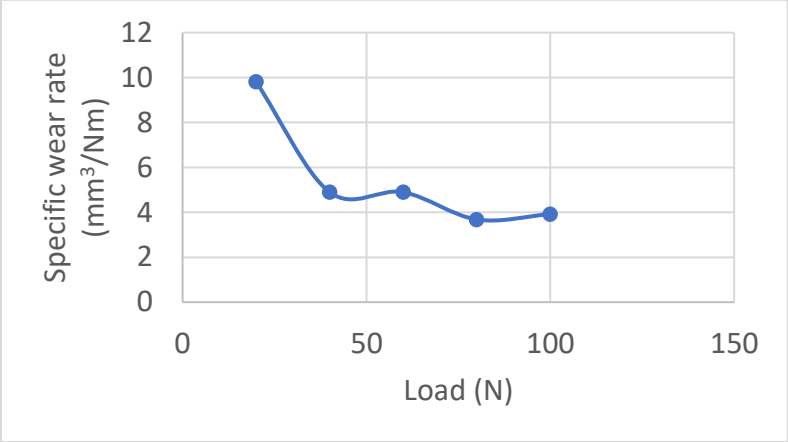

Figure 3: Specific wear rate vs load for 8 mm specimen at 2 m/s

Figure 4 presents the variation of the coefficient of friction with applied load. The coefficient of friction remains relatively stable, ranging from 0.55 to 0.59, with no significant dependence on load. This suggests the establishment of a steady-state sliding condition, possibly due to the formation of a stable mechanically mixed layer at the contact interface, which regulates frictional behavior despite increasing normal load.

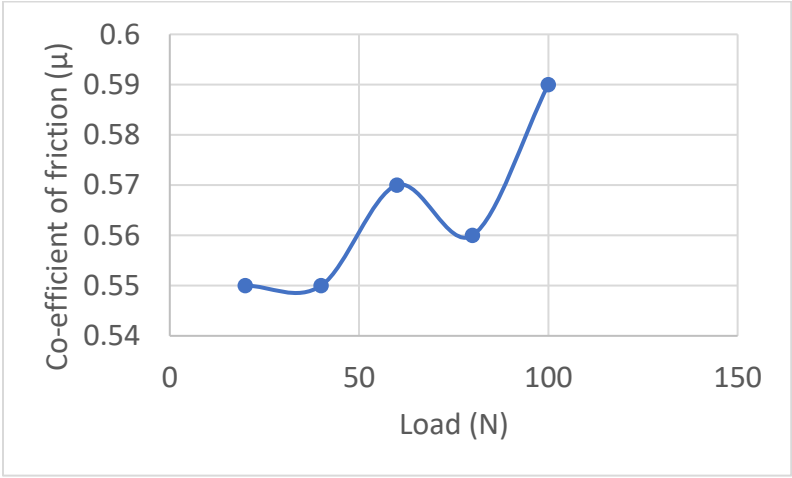

Figure 4: Co-efficient of friction vs load for 8 mm specimen at 2 m/s

https://doi.org/10.71058/jodac.v10i01010

The dimensionless wear coefficient as a function of load is shown in Figure 5. At lower loads (10–20 N), the wear coefficient exhibits higher values, approximately 6.64×10^{-5}, which may be attributed to the initial running-in period characterized by unstable contact conditions and higher material removal. With further increase in load, the wear coefficient decreases and stabilizes within the range of 2.49×10^{-5} to 3.32×10^{-5} up to 100 N. This stabilization indicates the transition to a steady wear regime, where improved load-bearing capacity of the composite and stabilization of the tribolayer contribute to controlled and predictable wear behavior.

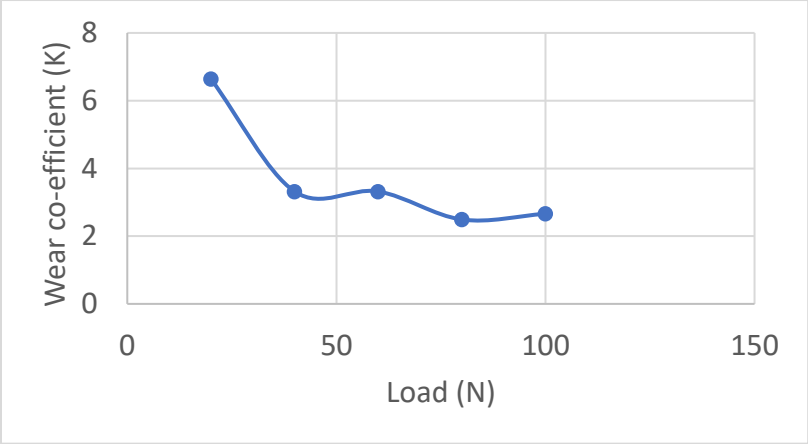

Figure 5: Wear co-efficient vs load for 8 mm specimen at 2 m/s

4.2 Wear analysis of 10 mm diameter pin specimen

The following discussion focuses on the trends observed for the 10 mm diameter pin specimen tested at a sliding velocity of 2 m/s.

Figure 6 illustrates the variation of wear rate with applied load. As the load increased from 10 N to 100 N, the wear rate increased from 0.000985 mm^3/m to 0.003942 mm^3/m, exhibiting a nearly linear trend. This behavior can be attributed to the increase in real area of contact between the mating surfaces due to plastic deformation of surface asperities under higher normal loads. The increased real contact area results in higher interfacial shear stresses, which facilitate material removal from the comparatively softer matrix during sliding, leading to an increased wear rate.

https://doi.org/10.71058/jodac.v10i01010

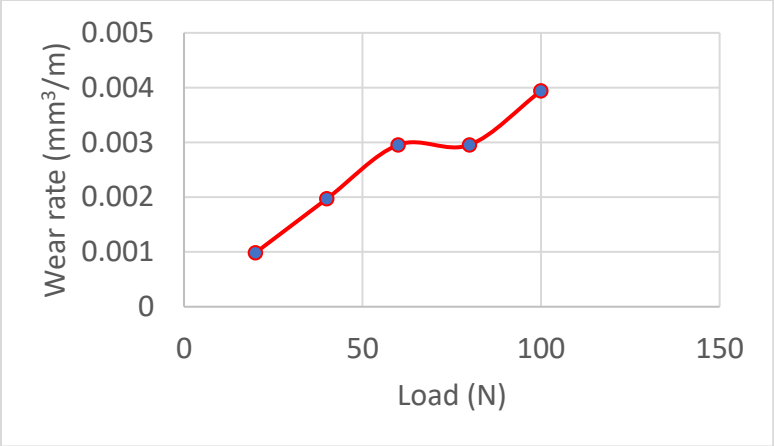

Figure 6: Wear rate vs load for 10 mm specimen at 2 m/s

The variation of specific wear rate with load is shown in Figure 7. Despite the increase in wear rate with load, the specific wear rate remains nearly constant, varying only between 3.7×10^{-5} and 4.93×10^{-5} mm³/Nm over the entire load range. This behavior is consistent with Archard's wear law, which states that wear volume is directly proportional to the applied load under mild wear conditions. When the wear volume increases linearly with load, normalization with respect to load and sliding distance results in an approximately constant specific wear rate, indicating that the dominant wear mechanism remains unchanged within the investigated load range.

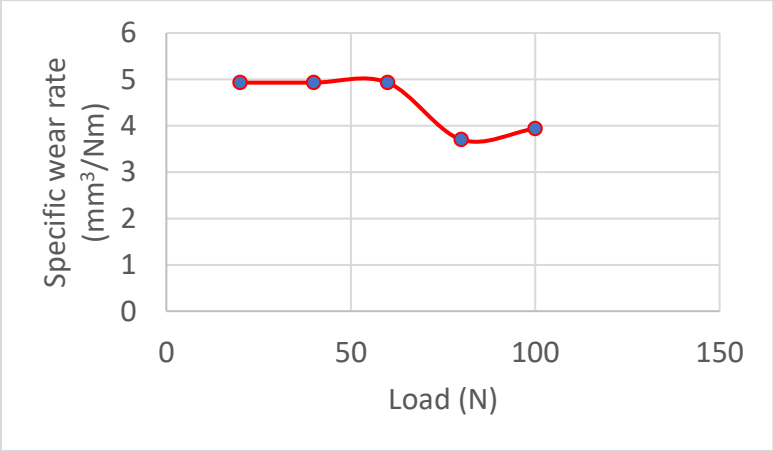

Figure 7: Specific wear rate vs load for 10 mm specimen at 2 m/s

Figure 8 presents the variation of the coefficient of friction with applied load. The coefficient of friction remains relatively stable, ranging from 0.48 to 0.57, with no significant dependence on load. This suggests the establishment of a steady-state sliding condition, possibly due to the formation of a stable mechanically mixed layer at the contact interface, which regulates frictional behavior despite increasing normal load.

https://doi.org/10.71058/jodac.v10i01010

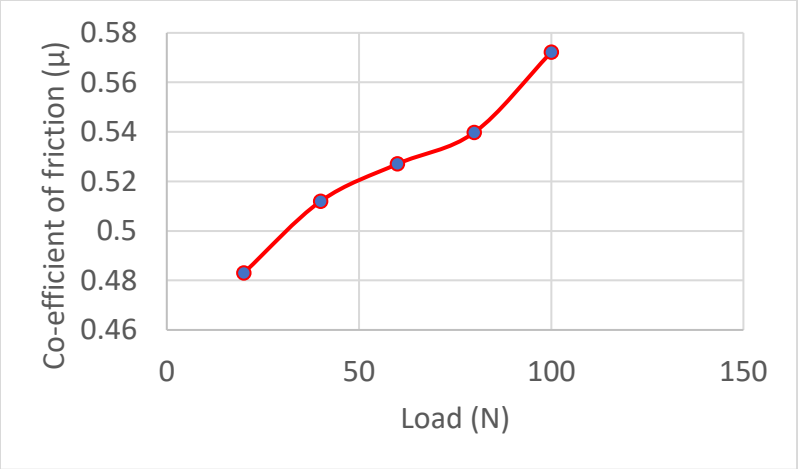

Figure 8: Co-efficient of friction vs load for 10 mm specimen at 2 m/s

The dimensionless wear coefficient as a function of load is shown in Figure 9. Despite the increase in wear rate with load, the wear co-efficient remains nearly constant, varying only between 2.5×10^{-5} and 3.33×10^{-5} mm^3/Nm over the entire load range. This stabilization indicates the transition to a steady wear regime, where improved load-bearing capacity of the composite and stabilization of the tribolayer contribute to controlled and predictable wear behavior.

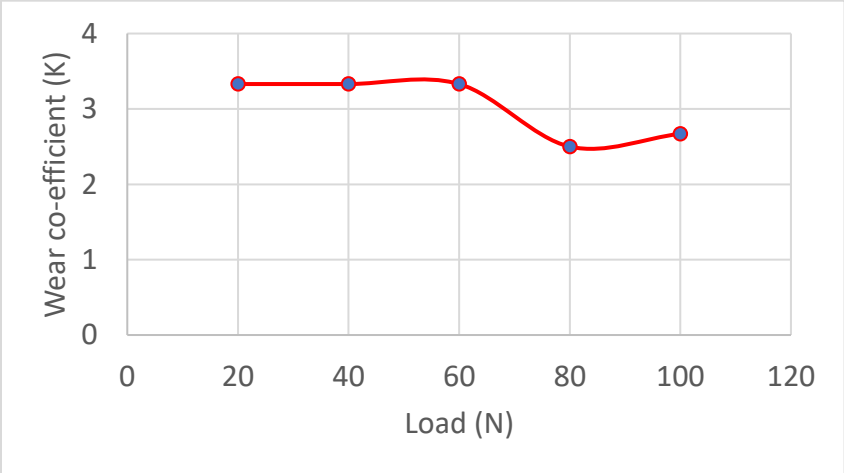

Figure 9: Wear co-efficient vs load for 10 mm specimen at 2 m/s

4.3 Comparative Discussion of Wear Parameters for 8 mm and 10 mm Diameter Pin Specimens

A comparative evaluation of the wear behavior of 8 mm and 10 mm diameter Al–Mg_2Si composite pins was conducted at an increased sliding velocity of 2 m/s under applied normal loads ranging from 20 N to 100 N. The superimposed variation of wear rate with load for both pin diameters at 2 m/s is presented in Figure 10. For both specimens, the wear rate increased progressively with increasing load, indicating load-dominated wear behavior. However, the 8 mm diameter pin consistently exhibited higher wear rates compared to the 10 mm pin throughout the investigated

https://doi.org/10.71058/jodac.v10i01010

load range. At the maximum applied load of 100 N, the wear rate of the 8 mm pin was approximately 3.9×10^{-3} mm³/m, while the corresponding wear rate for the 10 mm pin was lower, around 3.94×10^{-3} mm³/m. The improved wear resistance of the 10 mm pin is attributed to its larger contact area, which reduces contact stress and limits severe plastic deformation and abrasive material removal even at higher sliding velocity.

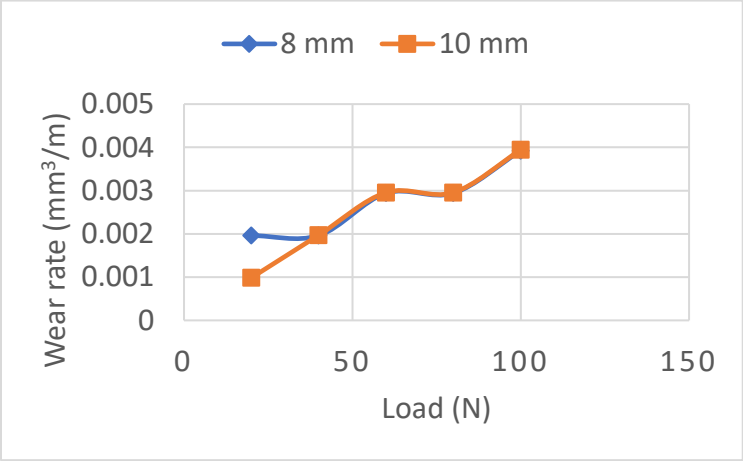

Figure 10: Comparison of wear rate vs load for 10 mm specimen at 2 m/s

The superimposed plot of specific wear rate versus load for both pin diameters at 2 m/s is shown in Figure 11. Despite the increase in absolute wear rate with load, the specific wear rate remained nearly constant for both specimens, varying within a narrow range of approximately $(3–10) \times 10^{-5}$ mm³/Nm. For the 8 mm pin, the specific wear rate decreased from about 9.8×10^{-5} mm³/Nm at 20 N to 3.9×10^{-5} mm³/Nm at 100 N, while the 10 mm pin consistently exhibited slightly lower values at corresponding loads. This near load-independent behavior confirms that the wear process continues to follow Archard's wear law even at higher sliding velocity, indicating that the fundamental wear mechanism remains unchanged and stable.

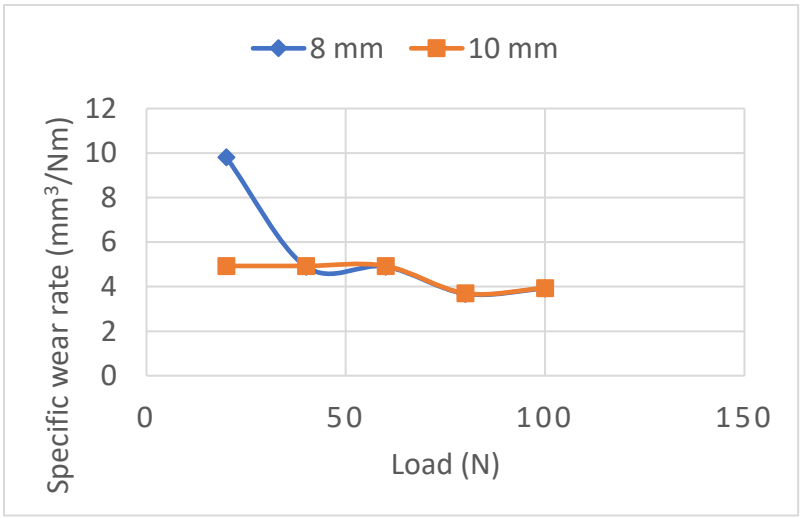

https://doi.org/10.71058/jodac.v10i01010

Figure 11: Comparison of specific wear rate vs load for 10 mm specimen at 2 m/s

The variation of coefficient of friction with applied load for both pin diameters at 2 m/s is illustrated in Figure 12. For both specimens, the coefficient of friction remained relatively constant with increasing load, with values lying in the range of approximately 0.48–0.59. The 10 mm pin generally exhibited marginally lower and more stable coefficient of friction values compared to the 8 mm pin. This behavior can be attributed to improved load sharing and the formation of a stable tribolayer at higher sliding velocity, which helps regulate interfacial shear stresses and frictional response.

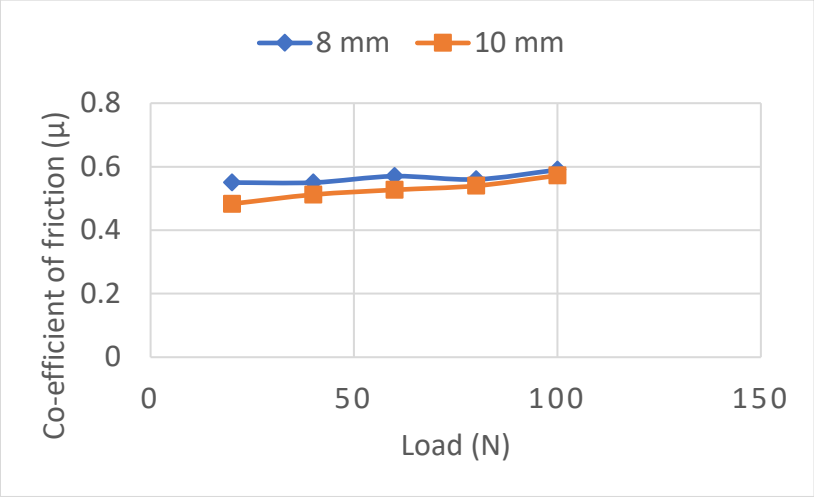

Figure 12: Comparison of co-efficient of friction vs load for 10 mm specimen at 2 m/s

The superimposed variation of the dimensionless wear coefficient with load at 2 m/s is presented in Figure 13. Higher wear coefficient values were observed at lower loads for both pin diameters, corresponding to the running-in wear regime characterized by unstable asperity interactions and surface adaptation. At low loads, the wear coefficient for the 8 mm pin was approximately 6.6×10^{-5}, whereas for the 10 mm pin it was around 3.3×10^{-5}. With increasing load, the wear coefficient decreased and stabilized for both specimens, remaining in the range of $(2.5–3.3) \times 10^{-5}$ at higher loads. The consistently lower wear coefficient observed for the 10 mm pin further confirms its superior resistance to material removal under high-speed sliding conditions.

https://doi.org/10.71058/jodac.v10i01010

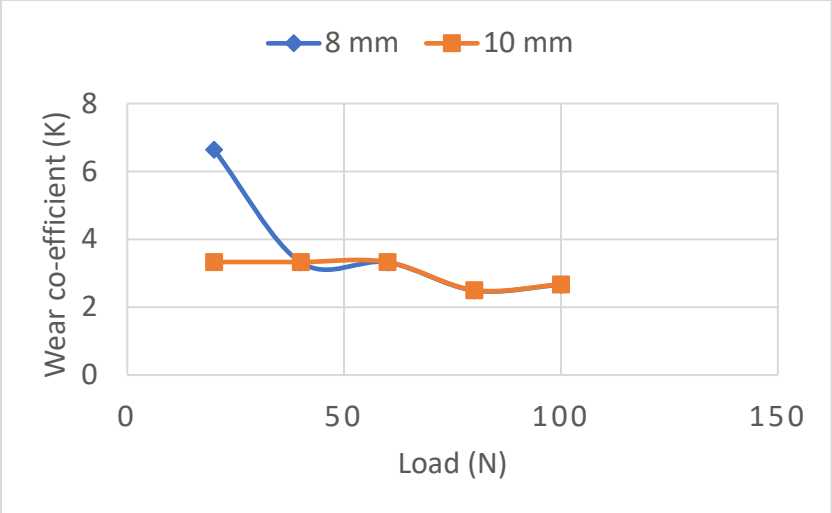

Figure 13: Comparison of wear co-efficient vs load for 10 mm specimen at 2 m/s

Overall, the comparative analysis of pin geometry reveals that the 10 mm diameter pins consistently exhibit lower wear rate and wear coefficient compared to the 8 mm pins at 2 m/s. The larger contact area associated with the 10 mm pins reduces nominal contact stress, thereby limiting plastic deformation and subsurface crack initiation. These findings highlight the significance of specimen geometry in controlling wear performance under high-speed sliding conditions.

5. Conclusions

The dry sliding wear behavior of in-situ Al–Mg_2Si composites at a sliding velocity of 2 m/s was systematically evaluated with respect to applied load and pin geometry. The results demonstrate that wear rate increases with increasing normal load due to enhanced plastic deformation and frictional heating at the contact interface. However, the specific wear rate remains nearly constant across the investigated load range, confirming the persistence of a stable wear mechanism consistent with Archard's wear theory. The coefficient of friction exhibits minimal sensitivity to load, indicating steady-state tribological behavior at higher sliding velocity. Comparative analysis shows that larger pin diameter results in lower wear rate and improved wear resistance due to reduced contact stress. Overall, the study confirms that in-situ Al–Mg_2Si composites possess stable and reliable wear performance under high-speed sliding conditions, making them suitable for demanding engineering applications involving elevated sliding velocities.

https://doi.org/10.71058/jodac.v10i01010

References

1. Hutchings IM, Shipway P. *Tribology: Friction and Wear of Engineering Materials*. 2nd ed. Oxford: Butterworth-Heinemann; 2017.
2. Blau PJ. *Friction Science and Technology: From Concepts to Applications*. 2nd ed. Boca Raton: CRC Press; 2009.
3. Sannino AP, Rack HJ. Dry sliding wear of discontinuously reinforced aluminium composites: review and discussion. *Wear*. 1995;189(1–2):1–19.
4. Alpas AT. Wear of aluminium alloys. *Tribol Int*. 2006;39(10):1213–1221.
5. Surappa MK. Aluminium matrix composites: challenges and opportunities. *Sadhana*. 2003;28(1–2):319–334.
6. Miracle DB. Metal matrix composites – From science to technological significance. *Compos Sci Technol*. 2005;65(15–16):2526–2540.
7. Lloyd DJ. Particle reinforced aluminium and magnesium matrix composites. *Int Mater Rev*. 1994;39(1):1–23.
8. Zhang Z, Chen DL. Consideration of Orowan strengthening effect in particulate-reinforced metal matrix composites. *J Mater Sci*. 2008;43:319–330.
9. Rohatgi PK, Asthana R, Das S. Solidification, structures, and properties of cast metal–ceramic particle composites. *Int Met Rev*. 1986;31(3):115–139.
10. Gupta M, Ling SNM. Magnesium, magnesium alloys, and magnesium composites. *Wiley*; 2011.
11. Kim YW, Chung DH. In situ synthesis of Mg_2Si particles in aluminium alloys. *Mater Sci Eng A*. 1995;198(1–2):125–132.
12. Ibrahim IA, Mohamed FA, Lavernia EJ. Particulate reinforced metal matrix composites — a review. *J Mater Sci*. 1991;26:1137–1156.
13. Archard JF. Contact and rubbing of flat surfaces. *J Appl Phys*. 1953;24(8):981–988.
14. Holm R. *Electric Contacts*. Berlin: Springer; 1946.
15. Straffelini G, Molinari A. Dry sliding wear of aluminium alloys. *Wear*. 2005;259(7–12):837–843.
16. Lim SC, Ashby MF. Wear-mechanism maps. *Acta Metall*. 1987;35(1):1–24.

https://doi.org/10.71058/jodac.v10i01010

17. Alpas AT, Zhang J. Effect of microstructure (grain size and second phase particles) on dry sliding wear of aluminium alloys. *Wear*. 1992;155(1):83–104.

18. Mondal DP, Das S. High stress abrasive wear behaviour of aluminium hard particle composites. *Wear*. 2005;258(1–4):521–532.

19. Zhang L, Xu H, Wang Y. Effect of sliding velocity on dry sliding wear behavior of aluminium matrix composites. *Tribol Int*. 2012;48:1–8.

20. Ghosh S, Sahoo KL. Influence of sliding speed and load on wear behaviour of aluminium-based composites. *J Mater Eng Perform*. 2014;23(6):2107–2115.

21. Prasad SV, Asthana R. Aluminum metal–matrix composites for automotive applications: tribological considerations. *Tribol Lett*. 2004;17(3):445–453.

22. Alpas AT, Embury JD. Sliding wear resistance of aluminium alloys. *Wear*. 1990;138(2):377–393.

23. Das S, Mondal DP. Dry sliding wear behaviour of aluminium matrix composites. *Mater Sci Eng A*. 2003;364(1–2):328–336.

24. Dwivedi SP, Sharma S, Mishra RK. Microstructure and wear behaviour of Al–Mg_2Si composites. *Tribol Int*. 2016;94:447–457.

25. Kumar A, Kumar S, Mukhopadhyay NK. Dry sliding wear behaviour of Al–Mg_2Si composites. *Wear*. 2017;376–377:1362–1371.

26. Straffelini G, Maines L. The role of load and speed on friction and wear of aluminium alloys. *Tribol Int*. 2013;64:198–205.

27. Alpas AT, Hu H. Formation and stability of mechanically mixed layers in sliding wear. *Wear*. 1999;225–229:121–133.

28. Kato K. Wear mechanisms. In: *Modern Tribology Handbook*. CRC Press; 2001. p. 327–361.

29. Suresh R, Krishna M. Effect of contact geometry on dry sliding wear of aluminium matrix composites. *Tribol Int*. 2015;82:318–327.

30. Dwivedi SP, Sharma S. Influence of pin diameter and sliding speed on wear of aluminium composites. *Wear*. 2014;318(1–2):240–247.